

Application of the Translated-SWE Algorithm for the Characterization of Antennas Installed on Cars Using a Minimum Number of Samples

F. Saccardi, F. Rossi, F. Mioc, L. J. Foged
Microwave Vision Italy SRL
Via dei Castelli Romani 59
00071, Pomezia, Italy
francesco.saccardi@microwavevision.com

P. O. Iversen
Orbit/FR Inc.,
506 Prudential Road
Horsham, 19044, PA, USA
peri@orbitfr.com

Abstract—Automotive antenna measurements are increasingly demanding. Modern cars are equipped with a large number of integrated antennas, spanning a wide frequency range for a large number of applications. Integrated antennas are strongly coupled with the structure, final testing are thus performed on the vehicle to accurately determine the performance. The physical and electrical size of typical cars, impose different measurement challenges while performing radiated testing in automotive Spherical Near Field (SNF) ranges. At higher frequencies, the coupling between antenna and vehicle is often limited to the near vicinity of the antenna. It is therefore customary to position the vehicle in the range such that the measurement coordinate system is centered on the antenna. The sampling requirement, to represent the antenna and nearby environment, can be reduced while maintaining acceptable accuracy. In many cases, such desirable arrangement becomes impractical, either due to a high number of antennas to be tested in different positions or due to size of the range. The Translated Spherical Wave Expansion (Translated-SWE) has recently been introduced as an advanced post-processing tool to place the local coordinate system in any position within the measurement range [1-2]. This eliminates the necessity to move the vehicle during testing.

In this paper, the Translated-SWE is applied to typical automotive measurements scenarios of antennas in displaced positions on vehicles. Sampling guidelines for full vehicle testing using this method are presented for the first time. Measurement accuracy is investigated experimentally on a 1:12 scaled vehicle with integrated antenna in a standard multi-probe system.

I. INTRODUCTION

The Translated Spherical Wave Expansion (Translated-SWE) has been recently proposed as a powerful Near Field to Far Field (NF/FF) transformation tool which allows to reduce the number of samples in offset spherical NF measurements [1-2]. The algorithm is based on the definition of a new reference system located on the Antenna Under Test (AUT) rather than on the center of the measurement sphere. The translation of the measurement reference system on the AUT allows to correctly represent the AUT with a minimum number of spherical modes (corresponding to a smaller minimum sphere) reducing the number of measured NF samples (down-sampling). The validation of the Translated-SWE have been presented in

previous publications in case of an AUT displaced along the Z-axis [1]. This may occur in case of mechanical constraints of the measurement system, such as the mast or stand-offs of fixed length, used to handle the AUT. The AUT can also be displaced intentionally with respect to the center of rotation to enhance the echo reduction capabilities of the modal filtering performed on the SWE spectrum [2]. In such scenarios, the Translated-SWE is very effective for echo reduction while significantly reducing the number of sampling points, due to the offset distance and thus the testing time. Techniques similar to the Translated-SWE have been also presented by other authors in [3-4].

The installation of antennas on complex structure, like cars, is another example of offset radiating devices. In many practical cases, reflections and scattering of the radiated fields are localized phenomenon. In such situations, a down-sampled acquisition can be performed taking advantage of the Translated-SWE, by moving the reference system on the fed antenna so that only the portion of structure surrounding that antenna is taken into account in the NF/FF transformation. The actual size of the measured structure is controlled by the sampling density.

The efficiency and accuracy of the Translated-SWE algorithm in the measurement of antenna on vehicles in severely offset positions is investigated in this paper. Measurements are performed on a patch antenna on a 1:12 scaled vehicle using a spherical multi-probe measurement system, MVG StarLab as shown in Figure 1.

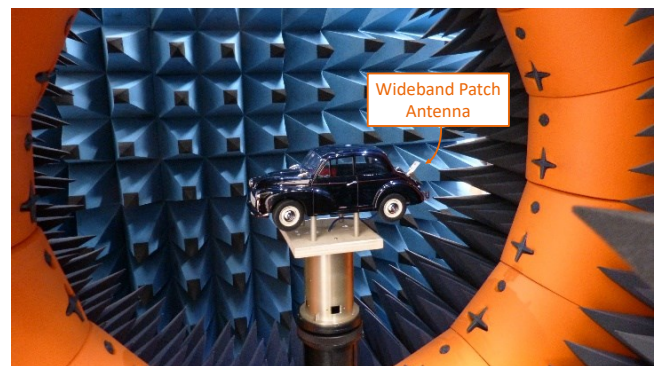


Figure 1. Measurement of a scaled car model in the MVG StarLab SNF system.

II. CLASSICAL AND TRANSLATED SWE

The description of the Translated-SWE algorithm is reported in this paragraph with a particular attention to the sampling criteria. In order to compare the properties of Translated-SWE with the standard spherical NF/FF transformation technique, the basic concepts of the SWE are also reported.

A. Spherical Wave Expansion

SWE is a known and established technique that allows NF/FF transformation in conventional Spherical NF (SNF) geometrical configurations [5-6]. When the SWE is applied, the measured field is projected over a set of orthogonal spherical wave basis functions in the computation of the Spherical Wave Coefficients (SWC). The FF is then evaluated combining the SWC with the spherical wave functions computed at infinite distance from the origin [6]. With reference to the drawing shown in Figure 2, the basic concepts of the SWE are recalled in this section.

Let us assume a spherical NF measurement with a measurement sphere radius (R_{MEAS}) and a corresponding Cartesian reference system (x, y, z) located in the center of the measurement sphere (see Figure 2). The sampling points on the measurement sphere are assumed to be equally spaced (constant $\Delta\theta$ angular sampling step).

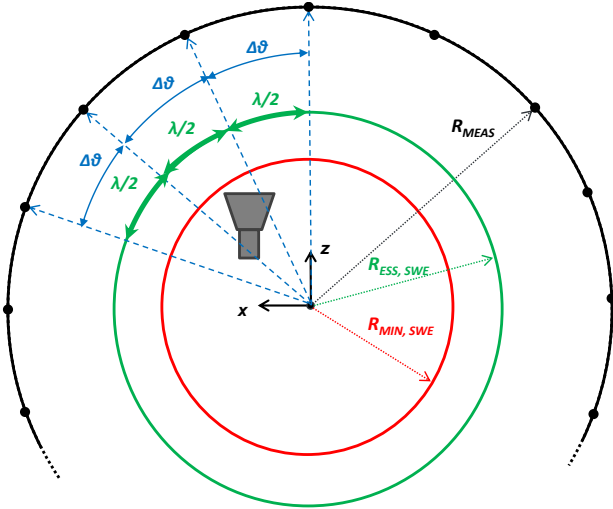


Figure 2. Offset spherical NF measurement: coordinate systems and sampling criteria of the standard-SWE.

An AUT is assumed to be located in a generic XYZ-offset configuration with respect to the (x, y, z) Cartesian reference system. With these assumptions, the SWE is typically performed involving the following Transmission formula [6]

$$w(A, \chi, \theta, \varphi) = 0.5 \sum_{\substack{smn \\ \sigma\mu\nu}} Q_{smn}^{(3)} e^{jm\varphi} d_{\mu m}^n(\theta) e^{j\mu\chi} C_{\sigma\mu\nu}^{sn(3)}(kA) R_{\sigma\mu\nu}^p \quad (1)$$

which expresses the complex signal received by a probe ($w(A, \chi, \theta, \varphi)$) of known coefficients ($R_{\sigma\mu\nu}^p$) as a function of the

probes coordinates and orientation, when an AUT, described by its own SWC ($Q_{smn}^{(3)}$), is transmitting. The symbols $d_{\mu m}^n(\theta)$ and $C_{\sigma\mu\nu}^{sn(3)}(kA)$ are respectively, rotation and translation operators that, together with the two complex exponentials $e^{jm\varphi}$ and $e^{j\mu\chi}$, are used to build the spherical wave expansion functions at each measurement point/orientation. Once the spherical functions are built, the transmission formula can be solved by mean of the AUT coefficients involving the procedure described in [6]. It is remarked that, if the sampling is performed using a constant increment along both scanning axes (θ, φ) a double FFT can be applied to compute the SWE in a very efficient way.

The number of field samples needed to accurately compute the SWC depends on the AUT minimum sphere which is defined as the smallest sphere centered in the origin of the coordinate system fully enclosing the AUT [6]. Such an AUT minimum sphere is illustrated by the red circle shown in Figure 2 together with its radius ($R_{MIN,SWE}$). According to the Nyquist criteria, the equivalent sampling on the AUT minimum sphere should be at least half-wavelength ($\lambda/2$). Thus, let us define the Equivalent Sampling Sphere (ESS) as the sphere which gives the equivalent half-wavelength spacing according to the applied angular sampling ($\Delta\theta$). The ESS is illustrated by the green circle in Figure 2 together with its radius ($R_{ESS,SWE}$) which is given by,

$$R_{ESS,SWE} = \frac{\lambda}{2 \Delta\theta_{SWE}} = \frac{\pi}{k \Delta\theta_{SWE}} \quad (2)$$

$\Delta\theta_{SWE}$ must be chosen so that $R_{ESS,SWE} \geq R_{MIN,SWE}$, or inverting the formula in (2),

$$\Delta\theta_{SWE} \leq \frac{\pi}{k R_{MIN,SWE} + n_{safety}} \quad (3)$$

where n_{safety} is an integer and positive number [6]. It is observed that the denominator of equation (3) corresponds to the maximum order of AUT radial modes (n-mode) of the transmission formula. When the AUT is located in an offset position, $R_{MIN,SWE}$ in equation (3) is greater, therefore a denser sampling step ($\Delta\theta_{SWE}$) must be considered in order to correctly compute the SWC.

B. Translated-SWE

The Translated-SWE (TSWE) is an advanced NF/FF transformation technique applicable to SNF measurement with offset AUT. As already pointed out and demonstrated in [1], the advantage of using Translated-SWE in case of offset AUT is the reduction of the number of NF samples to be measured with respect to the conventional Nyquist criteria.

Assuming the same spherical NF measurement layout described in the previous section, the Translated-SWE is based on the definition of a new reference system centered on the AUT rather than on the origin of the measurement sphere. The new reference system (x', y', z') allows to obtain the AUT minimum sphere shown in Figure 3.

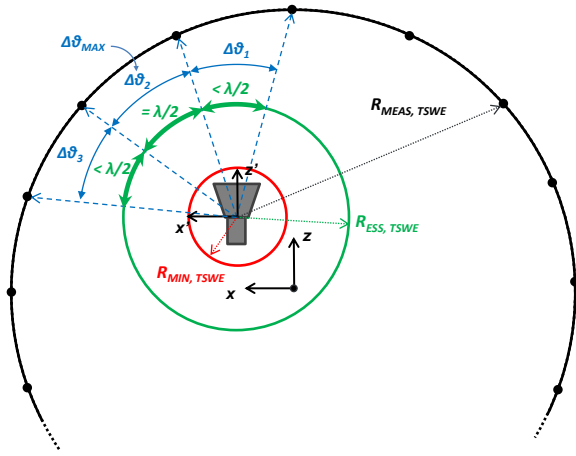


Figure 3. Offset spherical NF measurement: coordinate systems and sampling criteria of the Translated-SWE.

The radius of this new minimum sphere is $R_{MIN,TSWE}$ and, as can be easily noticed, is smaller than $R_{MIN,SWE}$ because it does not include the AUT offset distance. Therefore, a reduced sampling rate can be applied using Translated-SWE. However, a minimum sampling criterion of the Translated-SWE cannot be established from equation (3).

In the following we will refer to a displacement along Z-axis for simplicity, For a generic offset along the XY-axis the same deductions gathered for step $\Delta\theta$ can be applied to step $\Delta\phi$. As sketched in Figure 3, starting from a constant angular step $\Delta\theta$ relative to the reference system (x, y, z) , non-equally spaced samples ($\Delta\theta_1 \neq \Delta\theta_2 \neq \Delta\theta_3 \neq \dots$) are generated in the reference system (x', y', z') when its origin is moved outside the centre of the measurement sphere (it should be noted that this can be avoided considering an optimal sampling scheme [4], [7]). The drawback of such approach are the resulting size of the ESS and the complexity of the Translated-SWE algorithm.

When the Translated-SWE is applied the radius of ESS ($R_{ESS,TSWE}$) is given by the equation (4).

$$R_{ESS,TSWE} = \frac{\lambda}{2 \Delta\theta_{MAX}} = \frac{\pi}{k \Delta\theta_{MAX}} \quad (4)$$

$\Delta\theta_{MAX}$ is the maximum angular step in the reference system (x', y', z') . $\Delta\theta_{MAX}$ ensure, that all the equivalent samples on the ESS have a maximum spacing of half-wavelength (see Figure 3). Comparing equation (4) and equation (2), it is clear that $R_{ESS,TSWE}$ is reduced by a factor (α) given by (5).

$$\alpha = \frac{\Delta\theta}{\Delta\theta_{MAX}} \approx \left(1 - \frac{|offset|}{R_{MEAS}}\right) \leq 1 \quad (5)$$

In (5), $|offset|$ is the distance between the two reference systems. It should be noted that the α -factor is purely geometric and it depends on the offset distance and measurement radius (α decreases for bigger offsets and smaller measurement radius). The α -factor corresponds to the oversampling to be applied to the SNF offset measurements to be processed with Translated-SWE. The sampling step to be considered ($\Delta\theta_{TSWE}$) is thus given by (6).

$$\Delta\theta_{TSWE} \leq \alpha \left(\frac{\pi}{k R_{MIN,TSWE} + n_{safety}} \right) \quad (6)$$

As mentioned above the non-equally spaced measured samples at the distances $R_{MEAS,TSWE}$ in the new coordinate system increase the complexity of the expansion. In order to solve the transmission formula, the translation coefficient ($G_{\sigma\mu\nu}^{sn(3)}(kA)$) must be evaluated at different distances (see $R_{MEAS,TSWE}$ in Figure 3) respect to the classical SWE, where they are computed at a single distance. Moreover, it is not possible to take advantage of the double FFT. More specifically, if the offset is along the Z-axis, only the θ -axis will be non-equally spaced in the reference system (x', y', z') . In such case a matrix inversion (needed for the θ -axis) can be combined with FFT (for the ϕ -axis). Instead, if the offset is along X- and/or Y-axis (as in the present work), both the θ - and ϕ -axis will be non-equally spaced in the reference system (x', y', z') , resulting in a more computationally expensive solution, which involves a full-matrix inversion.

III. MEASUREMENT OF THE SCALED CAR MODEL

To validate the Translated-SWE algorithm as NF/FF transformation tool for automotive measurements of AUT in offset position, a scaled car model has been measured in the MVG StarLab portable multi-probe system [8].

A. Test case description

The car considered for the measurement is the 1:12 scaled model of the Morris Minor 1000 of 1965 shown in Figure 1. The dimensions of the scaled car are approximately: L x W x H = 31.3 x 12.9 x 12.7 cm (original dimensions: L x W x H = 3.76 x 1.55 x 1.52 m).

A wideband patch antenna with omnidirectional pattern has been considered as AUT. The AUT has been installed on the rear hood of the car model as shown in Figure 1. The DUT (car model and patch antenna) has thus been measured in the MVG StarLab system (see Figure 1) in the in the frequency range 12-18 GHz. The radius of the StarLab system is 45 cm, thus such a scaled measurement corresponds to a virtual automotive measurement in a multi-probe system of radius 5.4 m in the 1.0-1.5 GHz frequency range.

It should be noted that MVG multi-probe automotive ranges are characterized by a truncation of typically $\pm 80^\circ$ or $\pm 70^\circ$ in elevation [9-10]. The elevation truncation of the StarLab used in the measurements is much smaller $\pm 22.5^\circ$. In order to emulate a realistic automotive measurement, the same truncation of the automotive systems should be forced by properly removing NF points in the corresponding scan area. However, as described in [11], truncation errors are less important sources of error at higher frequencies, such as the frequencies reported in these validation experiments. In order to investigate accurately the issue of the sampling, which is critical at higher frequencies, the large truncation of the scanning area has not been introduced in this validation.

B. Measurement sampling

Figure 4 shows the (x, y, z) reference systems located in the center of the measurement sphere. As can be seen the DUT has been mounted in the StarLab with its bigger dimension aligned with the X-axis. The DUT is centered with respect to the Y-axis while is slightly offset along x (approx. -2.5 cm). The car roof is approximately at $z = 5$ cm. The patch antenna is approximately located at $(x, y, z) = (-15.5, 0, 0)$ cm.

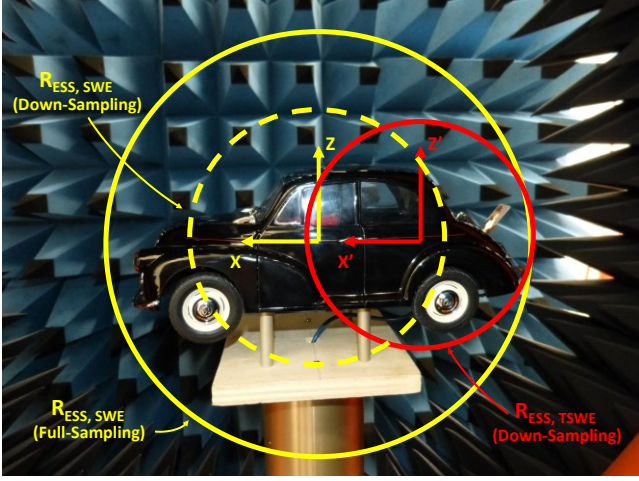


Figure 4. Illustration of the reference systems and Equivalent Sampling Spheres.

The radius of the minimum sphere enclosing the DUT (car model and patch antenna) is roughly 20.5 cm (12.5λ at 18 GHz). By applying equation (3) at the highest frequency of 18 GHz, the maximum θ and ϕ sampling steps needed to accurately compute SWE of the whole DUT is approximately $\Delta\theta = \Delta\phi = 2.0^\circ$. The radius of the ESS obtained using SWE with such a sampling ($R_{ESS,SWE}$) is illustrated by the solid yellow circle shown in Figure 4. As can be seen the DUT is fully enclosed in such an ESS.

In order to reduce the number of samples, it is assumed that only the portion of the scaled model of the car around the patch antenna is radiating, neglecting the coupling with the remaining part of the car. A reduced minimum sphere with a radius of 10 cm (roughly half of the full minimum sphere) has been considered. The primed reference systems has been located at $(x, y, z) = (-9, 0, 0)$ cm, which is approximately the geometrical center of the portion of the car located in the negative X-axis (see red reference systems in Figure 4). According to equations (5) and (6), the maximum θ and ϕ sampling step needed to measure such an offset minimum sphere with TSWE is approximately: $\Delta\theta = \Delta\phi = 3.8^\circ$. The radius of the ESS obtained using TSWE with such a sampling ($R_{ESS,TSWE}$) is illustrated by the solid red circle shown in Figure 4. As can be seen, the portion of the DUT nearby the source antenna is enclosed in such ESS.

Two measurements have been performed:

- “Full-sampling”: $\Delta\theta = \Delta\phi = 1.5^\circ$
- “Down-sampling”: $\Delta\theta = \Delta\phi = 3.75^\circ$

The radius of the ESS at each test frequency for the two measurements are reported in Table 1.

As can be seen in the second column ($R_{ESS,SWE}, \Delta\theta = \Delta\phi = 1.5^\circ$) of Table 1, the first measurement is over-sampled with respect to the minimum required sampling ($\Delta\theta = \Delta\phi = 2^\circ$). Such measurement has thus been processed with the standard SWE and considered as reference.

The second measurement is approximately 3.5 times down-sampled with respect to the conventional minimum sampling criteria ($91 * 180 = 16380$ sample points over the full sphere, against $49 * 96 = 4704$). As can be seen in the third column ($R_{ESS,SWE}, \Delta\theta = \Delta\phi = 3.75^\circ$) of Table 1, at higher frequencies, such a sampling rate is not enough if the standard SWE is used. This condition is also illustrated by the dashed circle in Figure 4. As can be seen, the radiating source is located outside the ESS. Therefore, inaccurate results are expected by the processing of the down-sampled measurement with the SWE, especially at higher frequency.

TABLE I. RADIUS OF THE ESS AT TEST FREQUENCIES (IN CM).

Frequency (GHz)	$R_{ESS,SWE}^a$ ($\Delta\theta = \Delta\phi = 1.5^\circ$)	$R_{ESS,SWE}^a$ ($\Delta\theta = \Delta\phi = 3.75^\circ$)	$R_{ESS,TSWE}^b$ ($\Delta\theta = \Delta\phi = 3.75^\circ$)
12	47.8	19.1	15.3
13	44.1	17.6	14.1
14	40.9	16.4	13.1
15	38.2	15.3	12.2
16	35.8	14.3	11.5
17	33.7	13.5	11.8
18	31.8	12.7	10.2

^a Obtained inverting equation (3) with $n_{safety} = 0$.

^b Obtained inverting equation (6) with $n_{safety} = 0$ ($\alpha = 0.8$).

ESS of the down-sampled measurement processed with TSWE are reported in the fourth column ($R_{ESS,TSWE}, \Delta\theta = \Delta\phi = 3.75^\circ$) of Table 1. As can be seen, ESS are smaller with respect to the corresponding ESS obtained processing the down-sampled measurement with the SWE, because they are translated in order to sample the portion of the car around the radiating source ($R_{ESS,TSWE} = \alpha R_{ESS,SWE}$).

C. Measurement results

The down-sampled measurement has been processed with both SWE and Translated-SWE (TSWE) and compared with the reference. It is remarked that the TSWE has been evaluated locating the primed reference system at $(x, y, z) = (-9, 0, 0)$ cm. As explained above and illustrated in Figure 4, when the TSWE is applied, part of the DUT is filtered out by the ESS. In order to have a reference result with the same filtering properties of TSWE, a modal filtering combined with a proper FF phase shift has been applied to the full-measurement. The applied spatial filter is equivalent to the red circle shown in Figure 4.

A global (full sphere) radiation pattern comparison is performed in term of Equivalent Noise Level (ENL), which is expressed by the following formula:

$$ENL = 20 \log_{10} \left(\text{mean} \left| \frac{E(\theta, \varphi) - \tilde{E}(\theta, \varphi)}{E(\theta, \varphi)_{MAX}} \right| \right) \quad (7)$$

In (7), $E(\theta, \varphi)$ is the reference pattern and $\tilde{E}(\theta, \varphi)$ is the reconstructed pattern. The ENL over the full sphere at each test frequency is shown in Figure 5.

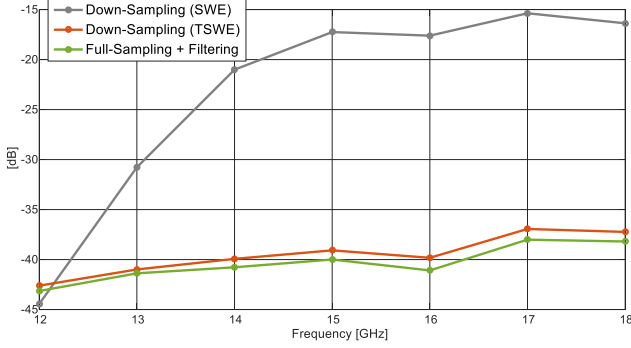


Figure 5. ENL with frequency obtained with different NF/FF processing.

The grey trace is the ENL of the down-sampled measurement processed with standard SWE. As expected, the performance is poor (> -20 dB) at higher frequencies where the source antenna is located outside the ESS (see Table 1). The ENL of the down-sampled measurement processed with the TSWE is shown by the orange trace and it is -37 dB in the worst case. A good agreement with reference is obtained. Finally, the green trace is the ENL of the spatial filtered (full-sampled) measurement. As can be seen the latter is -38 dB in the worst case, meaning that the coupling with the filtered part of the car can be considered negligible. Furthermore, orange and green traces are pretty close to each other, meaning that the errors introduced by the TSWE mainly due to the spatial filtering made by the ESS itself.

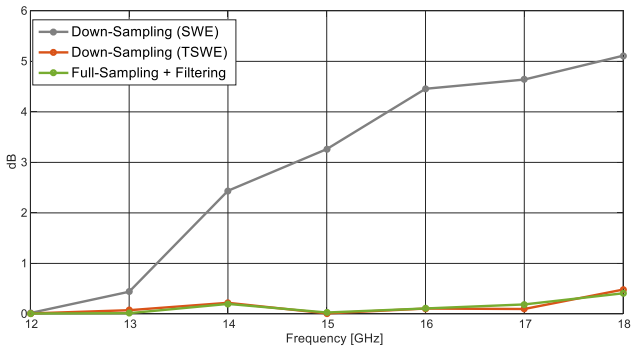


Figure 6. Measured peak directivity error with frequency obtained with different NF/FF processing.

The error on peak directivity obtained by the different processing of the two measurements is shown in Figure 6 at the different frequencies. As can be seen, TSWE and spatial filtered

directivity (orange and green traces respectively) give a maximum error of just below 0.4 dB at the highest frequency. As expected, the error on peak directivity obtained processing the down-sampled measurement with standard SWE (grey trace) is elevated for frequencies higher than 13 GHz, where the ESS is too small.

The comparison of the total directivity pattern between the reference and the down-sampled measurement processed with TSWE are shown in Figure 7 to Figure 9. The selected frequency for this comparison is 18 GHz, the highest and thus most critical. The vertical cut at $\varphi = 0^\circ$ (the one along the largest DUT dimension) is shown in Figure 7, while the vertical cut at $\varphi = 90^\circ$ is shown in Figure 8. The horizontal cut at $\theta = 90^\circ$ is instead reported in Figure 9.

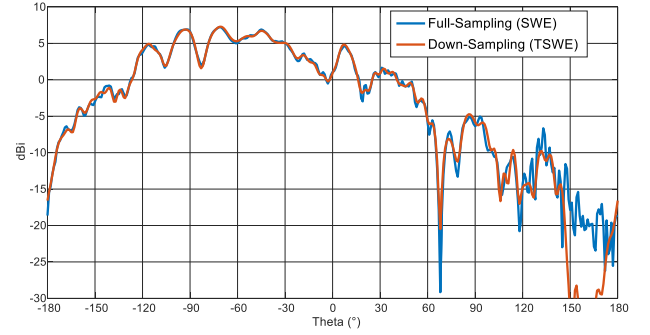


Figure 7. Directivity pattern comparison at 18 GHz (total field); vertical cut at $\varphi = 0^\circ$.

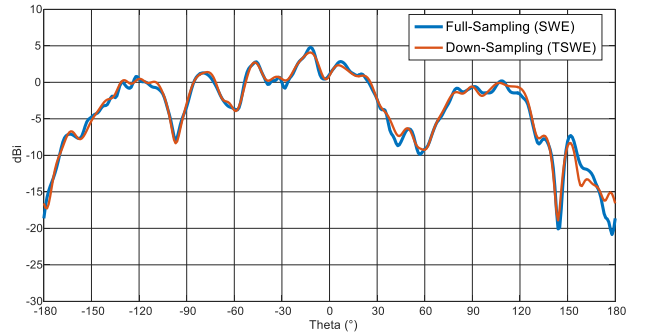


Figure 8. Directivity pattern comparison at 18 GHz (total field); vertical cut at $\varphi = 90^\circ$.

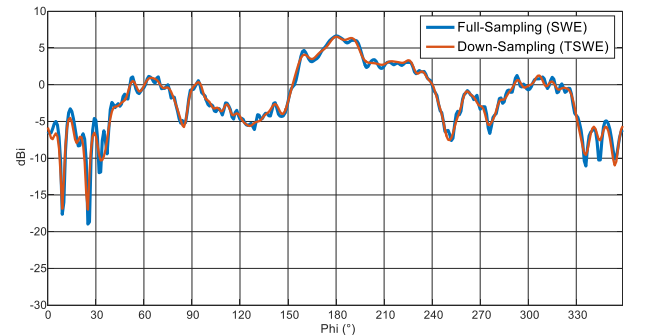


Figure 9. Directivity pattern comparison at 18 GHz (total field); horizontal cut at $\theta = 90^\circ$.

As can be seen, a good agreement is achieved in all the presented pattern comparison. The differences are associated to the ESS of the TSWE, which, as explained before, acts as a spatial filter. The “fast” ripple present in the reference pattern, originates from scattering with the car structure at large distance from the source. This is not included in the ESS and is thus filtered out in the down-sampled measurement processed with the TSWE. It should be noted that the interaction with the car structures far away from the source are due to the very low directivity of the AUT (approx. 4-5 dBi). Furthermore, as can be seen in Figure 7 and Figure 8, for approximately $\theta > 150^\circ$, the interaction with the supporting mast is filtered out in case of down-sampled measurement processed with TSWE. A better agreement of the pattern is thus expected by considering more directive antennas.

Comparison between the reference and the down-sampled measurement processed with TSWE in terms of radial and azimuthal spherical wave modes [6] is shown in Figure 10. It should be noted that, in order to compare the two spectra in the same reference system, a mathematical back-translation has been applied on the SWC [6] computed with TSWE. After the back-translation both spectra are centered in the (x, y, z) reference system. The agreement on the radial modes is very good down to -35 dB level while the azimuthal modes agree well even up to -45 dB level. Once again, the differences are due to the spatial filtering introduced by the ESS of the TSWE.

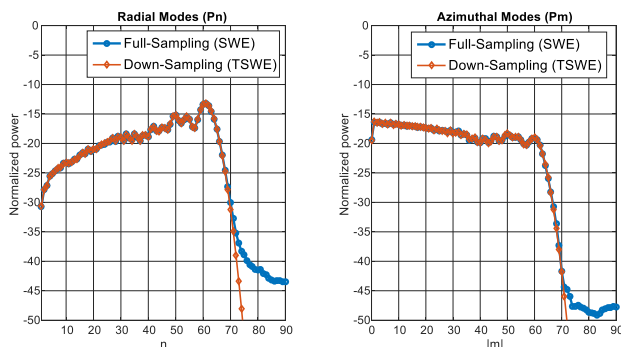


Figure 10. Spherical wave spectrum comparison at 18 GHz.

IV. CONCLUSIONS

Translated-SWE algorithm has been applied to spherical NF measurements of an antenna installed on a 1:12 scaled car model. A low directive patch antenna has been installed on the rear hood of the car in an offset position with respect to the center of the measurement sphere. The DUT has been measured in MVG portable multi-probe StarLab system in the 12-18 GHz frequency range. A reference measurement has been performed considering the conventional minimum sampling criteria corresponding to the entire DUT. A 3.5-fold down-sampled measurement has also been performed and processed with the TSWE algorithm to compute the FF. A translation along the X-axis has been considered during the application of the TSWE in order to include the most significant radiating part of the DUT.

Comparison in terms of Equivalent Noise Level, peak directivity and radiation pattern over the full sphere has shown very good agreements between reference and down-sampled measurement processed with TSWE, for each considered frequency. The small differences observed are due to the reduced size of the translated ESS defined by the TSWE, which act as a spatial filter.

REFERENCES

- [1] L. J. Foged, F. Saccardi, F. Mioc, P. O. Iversen “Spherical Near Field Offset Measurements Using Downsampled Acquisition and Advanced NF/FF Transformation Algorithm”, EUCAP 2016, Davos, Switzerland
- [2] F. Saccardi, L. J. Foged, F. Mioc, P. O. Iversen, “Echo Reduction with Minimum Sampling in Spherical Near Field Measurements using Translated-SWE Algorithm”, AMTA 2016, October 30 – November 4, Austin, TX, USA
- [3] R. Cornelius, D. Heberling and D. Pototzki, “Spherical Near-Field Far-Field Transformation with Infinite Ground Plane At Arbitrary Height z ”, EuCAP 2017, 19-24 March, Paris, France
- [4] Francesco D’Agostino, Flaminio Ferrara, Claudio Gennarelli, Rocco Guerriero, Massimo Migliozi, “A NF/FF Transformation with Spherical Scan for a Noncentred Quasi-Planar Antenna Using a Minimum Number of Data” EuCAP 2017, 19-24 March, Paris, France
- [5] IEEE Std 1720-2012 “Recommended Practice for Near-Field Antenna Measurements”
- [6] J. E. Hansen (ed.), Spherical Near-Field Antenna Measurements, Peter Peregrinus Ltd., on behalf of IEE, London, United Kingdom, 1988
- [7] F. D’Agostino et al. “Far-Field Pattern Reconstruction from Near-Field Data Collected via a Nonconventional Plane-Rectangular Scanning: Experimental Testing”, International Journal of Antennas and Propagation. Vol. 2014, Pag- 1-9
- [8] MVG StarLab website: “http://www.mvg-world.com/en/products/field_product_family/antenna-measurement-2/starlab”
- [9] MVG automotive range website: “http://www.mvg-world.com/en/products/field_product_family/antenna-measurement-2/sg-3000F”
- [10] MVG automotive range website: http://www.mvg-world.com/en/products/field_product_family/antenna-measurement-2/sg-3000-m
- [11] F. Saccardi, F. Rossi, L. Scialacqua, L. J. Foged, “Truncation Error Mitigation in Free-Space Automotive Partial Spherical Near Field Measurements”, to be published at AMTA 2017, 15-20 October, Atlanta, GA, USA;